

NASA/TM- ⁻⁸⁰⁻ 208112

o Accor
8-13-82 B
10-82

NIS

INFLUENCE OF MICROSTRUCTURE ON
THE FATIGUE CRACK GROWTH OF A516 IN HYDROGEN

711-26-711

10-1982

by

HARRY F. WACHOB

HOWARD G. NELSON

Reprinted from:

Hydrogen Effects in Metals

Proceedings of the Third International Conference on Effect of Hydrogen on Behavior of Materials sponsored by the Physical Metallurgy and Mechanical Metallurgy Committees of The Metallurgical Society of AIME, the National Science Foundation, and the U.S. Air Force Office of Scientific Research, Moran, Wyoming, August 26-31, 1980.

I.M. BERNSTEIN and ANTHONY W. THOMPSON
Carnegie-Mellon University
Pittsburgh, Pennsylvania

CONFERENCE  PROCEEDINGS

The Metallurgical Society of AIME

INFLUENCE OF MICROSTRUCTURE ON
THE FATIGUE CRACK GROWTH OF A516 IN HYDROGEN

Harry F. Wachob
Failure Analysis Associates
Palo Alto, CA 94304
&
NASA-Ames Research Center

Howard G. Nelson
NASA-Ames Research Center
Moffett Field, CA 94035

Introduction

Some day hydrogen may be used as a viable energy storage and transport medium within the United States. Hydrogen gas may be used to dilute and extend our present methane supply as a blend or may even be used in its pure elemental form as a primary fuel (1). Independent of the methods of production, storage, and distribution, the interaction of hydrogen with its containment material will play an integral role in the success of a hydrogen energy program. Presently, the selection of hydrogen containment materials can be made such that the material will remain reasonably free from environmental degradation; however, costly alloying additions are required. Unfortunately, high alloy steels are economically prohibitive when large-scale hydrogen energy storage, transmission, and conversion systems are desired. Therefore, in order to implement such hydrogen energy systems in the future, existing low-cost materials must be improved via mechanical, thermal, or thermo-mechanical processing methods or new low-cost materials which are compatible with hydrogen must be developed.

Originally, low strength, low alloy steels at room temperature were thought to be immune to hydrogen gas embrittlement, since no sustained load crack growth is observed (2). However, results of Clark (3) in HY80 and Nelson (2) in SAE 1020 have shown that the fatigue crack growth rate can be greatly accelerated in the presence of hydrogen gas. In recent results reported by Louthan (4) and Mucci (5), the smooth bar fatigue life of an Al06B pipeline steel was reduced up to a factor of ten when the tests were performed in a 13.8 MPa hydrogen environment. These results suggest that the selection of material for structures designed to operate in hydrogen under cyclic loads must include consideration of hydrogen/metal fatigue interaction.

Although the hydrogen/metal fatigue interaction can be severe in low strength low alloy steels, the degree of degradation may be altered by the underlying ferrous microstructure. At present, no correlation between microstructure and degree of hydrogen susceptibility exists for low strength steels. However, in high strength steels, susceptibility to hydrogen embrittlement has been shown to be strongly sensitive to the metallurgical microstructure (6, 7). In addition, compositional effects and grain size can

modify any specific susceptibility (7). In general, the best environmental resistance seems to be provided by a well tempered martensitic or bainitic microstructure, which has been ausformed to produce refined plate sizes and finely dispersed array of fine carbides (8, 9). A spheroidized structure of uniformly dispersed carbides is second best (9, 10) with a normalized structure being the poorest (9). Unfortunately, a similar ranking is not available for medium and low strength low alloy steels.

The objective of the current research program was to determine the role of ferrous microstructure on the near threshold fatigue crack growth rate for a low to medium strength low alloy steel. From these results, one can then identify the ferrous microstructure which is least susceptible to hydrogen degradation.

Experimental Procedure

Materials

Alloy A516-G70 plate chosen as a representative steel for this research program, was heat treated to obtain a variety of mechanical properties and microstructures. The plate, 1.25cm thick, was austenitized at either 900°C or 1200°C for 45 minutes, then icewater quenched, isothermally quenched, or furnace fan cooled. Some austenizing treatments were followed by tempering at 450°C for 1.5 hours. The ambient mechanical properties, microstructures, and respective processing schedules are listed in Table I.

TABLE I. PROPERTIES OF HEAT TREATED A516

CONDITION	YS, MPa	TS, MPa	MICROSTRUCTURE
NORMALIZED AS RECEIVED 900 C	300	35	PEARLITE FERRITE
MARTENSITIC 1200 C 1WQ TEMPERED 1.5 hr @ 450 C	805	30	TEMPERED MARTENSITE AND BAINITE
NORMALIZED 1200 C	305	180	PEARLITE FERRITE
BAINITIC 1200 C 150 TEMPERED 1.5 hr @ 450 C	415	200	BAINITE WITH CONTINUOUS FERRITE AT GRAIN BOUNDARIES (10%)
MARTENSITIC 1200 C 1WQ TEMPERED 1.5 hr @ 450 C	820	200	TEMPERED MARTENSITE AND BAINITE

Testing Procedure

Tensile specimens and WOL - compact tension specimens (1.25cm thick) were cut from the as-received plate; the tensile axis was parallel to the long transverse rolling direction and the WOL specimens were in the L-T orientation.

Tests in high pressure hydrogen were performed using a stainless steel high pressure chamber. After the chamber was sealed and evacuated, it was purged and backfilled slowly with hydrogen. As part of each charging procedure, the high purity hydrogen was passed through a coil submerged in liquid nitrogen to lessen water and other active gas contaminants. The chamber valve was then closed upon reaching the desired pressure, and the specimen and crack opening displacement gage were allowed to come to equilibrium with the hydrogen environment for 8×10^3 seconds prior to initiating the test.

The fatigue crack growth tests were performed according to the guidelines of ASTM 647-78 (1978) (11) with the exception that the Newmann equation for stress intensity (12) was used as an alternative to the ASTM calculation. Fatigue tests were performed under constant crack opening displacement; this resulted in an ever decreasing load increment ΔP , ($P_{max} - P_{min}$), or ΔK as the crack front extended. This load decay, as a function of cycles, was monitored and later used in the data reduction program. The fatigue crack growth tests were performed using a 1Hz haversine waveform and a constant R ratio (P_{min}/P_{max}) of ~0.15. Variations in cyclic loading rate from 0.1 to 10Hz,

did not have a significant effect in air or in hydrogen.

Fractographic and metallographic was completed. If etching of was desired, a solution containing anol was used. This etching procedure microstructural features on the

Fatigue Crack Growth Results

The fatigue crack growth rate in a high pressure hydrogen environment. The FCGR increased and then high pressure hydrogen compared to air, the near-threshold fatigue austenitizing temperature or austenizing environment and microstructure are

Baseline fatigue tests were performed. Fatigue crack growth rates were measured (experimental resolution) and 10⁻⁶ m/cycle appeared to be independent of microstructure, as can be seen in Figure 3.8. Below $\Delta K = 16 \text{ MPa}\cdot\text{m}^{1/2}$, however, the FCGR level on the y-axis decreased, the FCGR decreases with increasing austenitizing temperature and 1200°C. Threshold values ($\pm 1 \text{ MPa}\cdot\text{m}^{1/2}$)

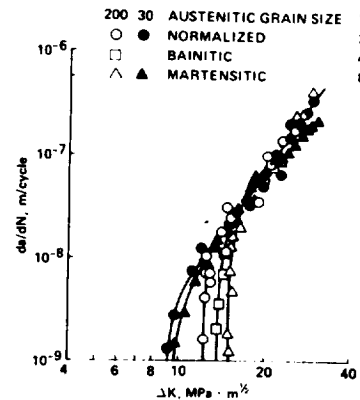


Fig. 1. The influence of austenitic grain size and yield strength on FCGR of A516 at R = 0.15 and v = 0.3 in air.

are tested in hydrogen. Also, the shape of the FCGR curves remain similar in hydrogen. Fig. 2.

FATIGUE CRACK GROWTH IN A516 705

did not have a significant effect on the observed fatigue crack growth rate in air or in hydrogen.

Fractographic and metallographic analyses were performed after testing was completed. If etching of the fracture surface or metallographic section was desired, a solution containing 4 grams of picric acid in 100 ml of methanol was used. This etching procedure permitted the delineation of several microstructural features on the fracture surface.

Results

Fatigue Crack Growth Results

The fatigue crack growth rate (FCGR) of this A516 steel was influenced by a high pressure hydrogen environment and by variations in ferrous microstructure. The FCGR increased and the fatigue threshold value (ΔK_0) decreased in high pressure hydrogen compared with those values obtained in air. In addition, the near-threshold fatigue behavior was strongly influenced by the final austenitizing temperature or austenitic grain size. Details for a given environment and microstructure are present below.

Baseline fatigue tests were performed in laboratory air (23°C and 45% RH). Fatigue crack growth rates were obtained between 10^{-9} m/cycle (lower limit of experimental resolution) and 10^{-6} m/cycle. At $\Delta K \approx 16 \text{ MPa}\cdot\text{m}^{1/2}$, the FCGR appeared to be independent of ferrous microstructure or austenitizing temperature, as can be seen in Figure 1. The slope of this linear regime in air is 3.8. Below $\Delta K = 16 \text{ MPa}\cdot\text{m}^{1/2}$, however, the effect of final austenitizing temperature and strength level on the crack growth behavior becomes apparent. As ΔK decreased, the FCGR decreases rapidly for those specimens austenitized at 1200°C. Threshold values ($\pm 1 \text{ MPa}\cdot\text{m}^{1/2}$) in air were $14 \text{ MPa}\cdot\text{m}^{1/2}$ for the martensitic structure, $13 \text{ MPa}\cdot\text{m}^{1/2}$ for the bainitic structure, and $12 \text{ MPa}\cdot\text{m}^{1/2}$ for the normalized ferritic-pearlitic structure. One important point to note is that the martensitic structure had the highest threshold value yet had a 50% higher yield strength than the normalized or bainitic structures.

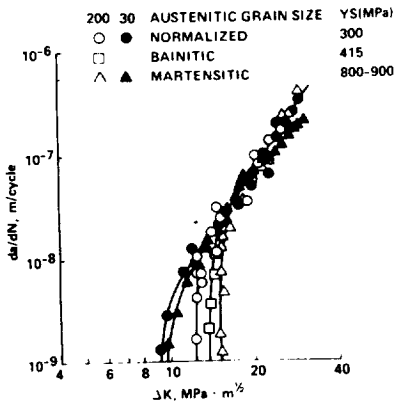


Fig. 1. The influence of austenitic grain size and yield strength on the FCGR of A516 at $R = 0.15$ and $\nu = 1 \text{ Hz}$ in air.

are tested in hydrogen. Also, the fatigue threshold values are lower in hydrogen than in air for all microstructures tested. The general features and shape of the FCGR curves remain similar to the air data as is indicated in Fig. 2.

Specimens austenitized at 900°C exhibit a linear crack growth behavior with ΔK above $\approx 11 \text{ MPa}\cdot\text{m}^{1/2}$ (Fig. 1). Below this limit, the FCGR drops abruptly and approaches threshold values of $9.5 \text{ MPa}\cdot\text{m}^{1/2}$ for the martensitic structure and $9 \text{ MPa}\cdot\text{m}^{1/2}$ for the ferritic-pearlitic structure. Again, a slightly higher threshold is obtained in the higher strength martensitic structure.

High pressure hydrogen is found to alter the fatigue behavior of the A516 steel as shown in Fig. 2. For a given ΔK , the FCGR increases above that observed in air when specimens

Above $\Delta K=13 \text{ MPa}\cdot\text{m}^{1/2}$ the FCGR in hydrogen appears to be independent of ferrous microstructure and prior austenitic grain size (Fig. 2). The slope of this linear ΔK curve is about 5.5 which is approximately 50% greater than the slope of 3.8 observed in air. As observed in air, the fatigue thresholds are higher for specimens austenitized at 1200°C than for those austenitized at 900°C . The threshold values for the 1200°C austenitized microstructure are $13 \text{ MPa}\cdot\text{m}^{1/2}$ for the martensitic structure, $11.5 \text{ MPa}\cdot\text{m}^{1/2}$ for the bainitic structure, and $10.5 \text{ MPa}\cdot\text{m}^{1/2}$ for the ferritic-pearlitic microstructure. The threshold values for the 900°C austenitizing microstructures are $9 \text{ MPa}\cdot\text{m}^{1/2}$ for the martensitic microstructure and $8 \text{ MPa}\cdot\text{m}^{1/2}$ for the ferritic-pearlitic microstructure. Similar to that observed in air, a slight increase in threshold occurs with increased yield strength.

Fractographic Results

The effect of hydrogen, as seen fractographically, was to reduce the features typically associated with plasticity. The failure mode in air was transgranular ductile tearing with evidence of fatigue striations. In hydrogen, the failure mode is either transgranular cleavage or intergranular separation. Two microstructures (ferritic-pearlitic normalized at 900°C and the martensitic austenitized at 1200°C) exhibit all of the various fractographic features and will be used as examples.

The greatest change in failure mode occurred for the 900°C normalized microstructure. The primary fractographic features after fatigue in air were ductile tearing and fatigue striation formation; secondary cracking along α -ferrite-pearlite interfaces; and out-of-plane crack initiation at MnS rolling inclusions. These features were developed in air over the entire ΔK range investigated (Fig. 1). However, as ΔK decreased, less overall gross plasticity was associated with the fracture surface.

In hydrogen, the fracture mode of the normalized specimens gradually changed from a transgranular cleavage (Fig. 3) failure at $\Delta K=24 \text{ MPa}\cdot\text{m}^{1/2}$ to an intergranular failure (Fig. 4) $\Delta K=9 \text{ MPa}\cdot\text{m}^{1/2}$.

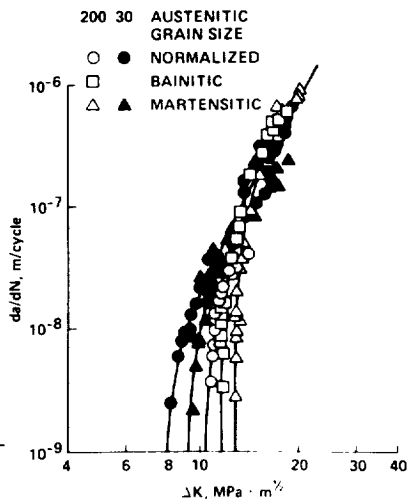


Fig. 2. The influence of austenitic grain size and microstructure on the FCGR of A516 at $R = 0.15$ and $v = 1 \text{ Hz}$ in 6.9 MPa hydrogen.

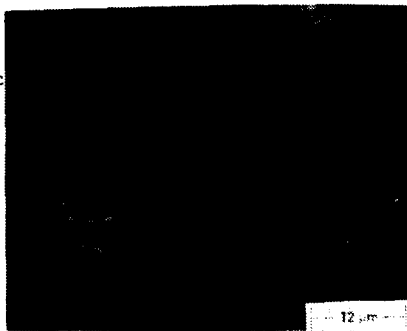


Fig. 3. Fractograph of the transgranular fracture of normalized A516 produced during fatigue at $\Delta K=24 \text{ MPa}\cdot\text{m}^{1/2}$ in $6.9 \text{ MPa}\cdot\text{H}_2$.

The majority of the intergranular failures occurred at ferrite boundaries. (The fracture surfaces have been etched to discern ferrite and pearlite regions). Evidence of gross plastic deformation, secondary cracking, and MnS inclusion was absent or substantially reduced in hydrogen.

In the 1200°C martensitic structure, the failure mode was primarily transgranular in both air and hydrogen. The fatigue surfaces produced in air show evidence of granular martensitic packets and minor amounts of intergranular and local areas of plastic deformation and striation formation. A fracture surface produced by fatigue in air is illustrated in Fig. 5. In hydrogen environment, the transgranular failures exhibited less plasticity as seen in Fig. 6. Addition of hydrogen increased the amount of intergranular separation slightly, but the total failure surface area was not significantly affected.

No microstructural comparisons were consistently associated with granular failures in the martensitic specimens. In the bainitic structure, however, intergranular separation was found to be associated with the pearlite-ferrite boundaries similar to that seen in the normalized material.

Discussion

The influence of microstructure on the FCGR of A516 steel in air parallels observations for a wide variety of carbon steels. The FCGR in hydrogen ΔK values are in good agreement with those for A516-G60 (13), A516-G70 (14), and A516-G70 (16). The threshold stress intensity for the normalized microstructure is similar to that for ferritic-pearlitic steels (13) and for the quenched and tempered steels with austenitic grain sizes.

However, Minakawa and Murakami (17) reported that the fatigue strength of ferritic-martensitic microstructures is in good agreement with that of ferritic-pearlitic and bainitic microstructures austenitized at 1200°C .

The majority of the intergranular failures occurred at ferrite-pearlite boundaries. (The fracture surfaces have been etched to discern ferrite and pearlite regions). Evidence of gross plastic deformation, secondary cracking, and MnS inclusion effects was absent or substantially reduced in hydrogen.

In the 1200°C martensitic microstructure, the failure mode was primarily transgranular in both air and hydrogen. The fatigue surfaces produced in air show evidence of transgranular martensitic packet failures, minor amounts of intergranular failure, and local areas of plastic deformation and striation formation. A typical fracture surface produced by fatigue in air is illustrated in Fig. 5. In a hydrogen environment, the transgranular failures exhibited less plasticity as seen in Fig. 6. Additionally, in hydrogen the amount of intergranular separation increased slightly to 10% of the total failure surface.

No microstructural component was consistently associated with intergranular failures in the martensitic specimens. In the bainitic microstructure, however, intergranular separation was found to be associated with the pearlite-ferrite boundary, similar to that seen in the 900°C normalized material.

Discussion

The influence of microstructure of A516 steel in air parallels previous observation for a wide variety of plain carbon steels. The FCGR in air at high ΔK values is in good agreement with the literature results on SAE 1020 (2), A516-G60 (13) A516-G70 (14), and several specially prepared Fe-C alloys (15-16). The threshold stress intensity value at 10^{-9} m/cycle for the 900°C normalized microstructure is very similar to that obtained for a variety of ferritic-pearlitic steels (15-16). No threshold data is presently available for the quenched and tempered martensitic structures or for the larger prior austenitic grain sizes.

However, Minakawa and McEvily (17) reported recently on a duplex ferritic-martensitic microstructure which had threshold values of $\Delta K_0 \approx 14 \text{ MPa}\cdot\text{m}^{1/2}$. This is in good agreement with the threshold values obtained for the martensitic and bainitic microstructures in the present study that were austenitized at 1200°C.

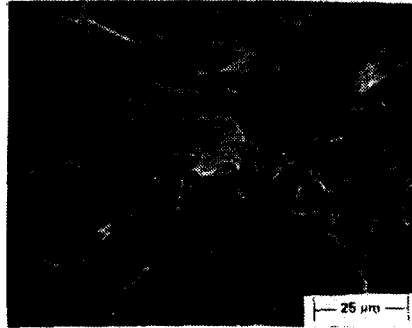


Fig. 4. Fractograph of intergranular separation of normalized A516 produced during fatigue at $\Delta K = 10 \text{ MPa}\cdot\text{m}^{1/2}$ in 6.9 MPa H_2 .

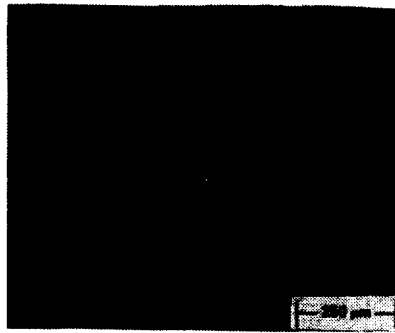


Fig. 5. Fractograph of the transgranular fracture of martensitic A516 produced during fatigue at $\Delta K = 24 \text{ MPa}\cdot\text{m}^{1/2}$ in air.

The fatigue crack growth behavior of A516 steel is greatly influenced by the presence of a high-pressure hydrogen environment. The FCGR is increased by as much as a factor of ten above that observed in air (Figs. 1 and 2). This is in good agreement with earlier results of Nelson (2) on a ferritic-pearlitic SAE 1020 steel. The threshold stress intensities for fatigue crack growth are also lowered in hydrogen compared with air for all microstructures investigated (Fig. 1 and 2). Ritchie has measured the fatigue threshold in 0.1 MPa (1 atm) hydrogen for an X-60 linepipe steel and reported a value of $5.9 \text{ MPa}\cdot\text{m}^{1/2}$ at 10^{-13} m/cycle (18). Additionally, he has also studied 2% Cr.-1Mo steel (19) and found $\Delta K=9 \text{ MPa}\cdot\text{m}^{1/2}$ at a crack growth rate of 10^{-9} m/cycle. Both materials were austenitized in the 900°C range. These results are in good agreement with the values measured in the present study for a ferritic-pearlitic microstructure austenitized at 900°C.

The decrease in threshold observed in hydrogen was more severe in the ferritic-pearlitic microstructures (12% decrease) than in the martensitic microstructures (6% decrease). The fact that martensitic microstructures exhibit higher thresholds and therefore have a higher resistance to early crack growth may be a partial explanation for the observed fact that in high strength steels, the best resistance to hydrogen in an aqueous environment is found in the well tempered martensitic and bainitic microstructures (8, 9). However, comparison of these results may not be valid, because the mechanisms of hydrogen degradation in the high strength steels under a static load may not be the same as for this low strength steel under dynamic loads. Further experimentation is required to fully understand the additional hydrogen resistance observed in these cyclic crack growth tests.

The single most important microstructural variable found in this study is the prior austenitic grain size. The fatigue threshold stress intensity value is increased with increasing austenitic grain size. This has been observed by others and is the general behavior for high strength steels (7), precipitation hardened ferrites (20), and plain carbon steels (16). Present results indicate the same trend occurs for the hydrogen fatigue threshold as well. In both air and hydrogen, the fatigue threshold is observed to increase a minimum of 25% for a factor of ten increase in austenitic grain size. Finally, these results suggest that in welded structures, material experiencing the lowest austenitizing temperatures, such as in the base plate or at the parent metal - HAZ interface, may initiate flaws earlier and at lower stress levels, than in that material which has experienced higher austenitizing temperatures such as in the HAZ and fusion zone.

Another parameter found to influence near threshold fatigue behavior is the strength level. In the present study as the strength level increases for a given austenitizing temperature, the threshold fatigue value also increases. This increase, although small, is found to exist in both air and hydrogen. This shift in threshold is contrary to what has been seen by others in both low-strength (16, 19, 20) and ultra-high strength steels (7). However, Minakawa and McEvily (17) have reported an increase in the threshold with in-

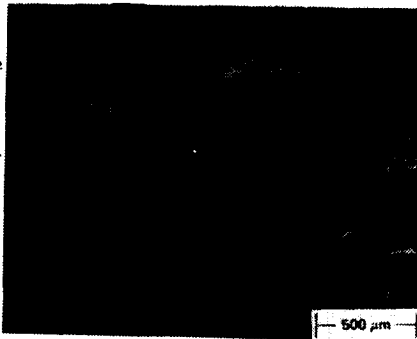


Fig. 6. Fractograph of the transgranular fracture of martensitic A516 produced during fatigue at $\Delta K \approx 15 \text{ MPa}\cdot\text{m}^{1/2}$ in 6.9 MPa H_2 .

creasing strength of duplex ferrite. It is suggested that a large crack closure effect and refinement of plastic deformation processes on the fracture surface analysis indicates that ΔK_{eff} is lower in duplex ferrous microstructures than in the present microstructure whereby less plastic deformation is required to strain the amount of plastic deformation. This constraint is also suggested by the processes on the fracture surface (Figs. 5 and 6). However, no measurements were made in this study to verify

Conclusions

Hydrogen has been shown to accelerate the fatigue behavior of a low strength, low alloy steel. Hydrogen accelerates the fatigue behavior of a low strength, low alloy steel. Hydrogen accelerates the threshold fatigue value as compared to air. The grain size dependence and a strain rate dependence of fatigue behavior, has also been observed with increased grain size and in-

From these results, martensitic microstructures provide the best fatigue behavior of A516 low alloy steel in air environments. On the other hand, a low austenitizing temperature and the lowest fatigue threshold are observed in air environments.

Acknowledgements

This program was partially supported by the Office of Advanced Conservation Branch.

1. W. W. Scherenbach, Proc. of 1st International Conference on Fracture, Contractor Review, pp. 67-74, American Nuclear Society, Washington, D.C., Nov. 27-30, 1978.
2. W. G. Clark, Jr., Hydrogen in Steels, eds., p. 149, TMS-AIME, New York, 1976.
3. H. G. Nelson, Proc. of 2nd International Conference on Fracture, Materials, pp. 690-699, Blacksburg, VA, October 1977.
4. M. R. Louthan, Jr., Annual Report on Fracture, Stress in Controlling Susceptibility to Fracture, Blacksburg, VA, October 1977.
5. J. Mucci, Final Report on "Hydrogen Transmission," Project 100, Florida State University, Tallahassee, Florida, May 1980.
6. I. M. Bernstein and A. W. McEvily, Hydrogen in Steels, eds., pp. 267-86, TMS-AIME, New York, 1976.

creasing strength of duplex ferritic-martensitic microstructures. They suggested that a large crack closure occurs due to back stresses and confinement of plastic deformation associated with the hard martensite. Their analysis indicates that ΔK_{eff} is approximately the same for the variety of duplex ferrous microstructures tested. A similar situation may exist in the present microstructure whereby the quenched and tempered microstructures constrain the amount of plastic deformation that can occur at the crack tip. This constraint is also suggested by evidence of reduced plastic deformation processes on the fracture surface of the quenched and tempered specimens (Figs. 5 and 6). However, no measurements of crack closure or effective ΔK were made in this study to verify their proposal.

Conclusions

Hydrogen has been shown to degrade the near-threshold fatigue properties of a low strength, low alloy steel and to be independent of ferrous microstructure. Hydrogen accelerates the fatigue crack growth rate and decreases the threshold fatigue value as compared to that observed in air. An austenitic grain size dependence and a strength level dependence of the near-threshold fatigue behavior, has also been observed. The fatigue threshold increases with increased grain size and increased yield strength.

From these results, martensitic microstructures produced at higher austenitizing temperatures provide the best static strength and near-threshold fatigue behavior of A516 low alloy steel in both high pressure hydrogen and air environments. On the other hand, the normalized microstructure produced at a low austenitizing temperature results in both the lowest static strength and the lowest fatigue threshold in both high pressure hydrogen and air environments.

Acknowledgements

This program was partially funded by the U. S. Department of Energy, Office of Advanced Conservation Technologies, Thermal and Chemical Storage Branch.

References

1. W. W. Scherenbach, Proc. of the DOE Chemical/Hydrogen Energy Systems Contractor Review, pp. 67-85, U.S. Department of Energy, Washington, D.C., Nov. 27-30, 1978.
2. W. G. Clark, Jr., Hydrogen in Metals, A. W. Thompson and I. M. Bernstein, eds., p. 149, TMS-AIME, New York, NY, 1974.
3. H. G. Nelson, Proc. of 2nd Int. Conference on Mechanical Behavior of Materials, pp. 690-699, Boston, August 1976.
4. M. R. Louthan, Jr., Annual Report on "The Roles of Rate and State of Stress in Controlling Susceptibility to Hydrogen Embrittlement," VPI&SU, Blacksburg, VA, October 1979.
5. J. Mucci, Final Report on "Evaluation of Laser Welding Techniques for Hydrogen Transmission," Pratt and Whitney Aircraft Group, West Palm Beach, Florida, May 1980.
6. I. M. Bernstein and A. W. Thompson, International Metals Reviews, Vol. 21, 1976, pp. 267-86.

7. R. O. Ritchie, Metal Science, 1977, Vol. 11, pp. 36881.
8. J. D. Hobson and C. Sykes, JISI, 1951, Vol. 169, p. 209.
9. E. Snape, Corrosion, 1968, Vol. 24, pp. 251-261.
10. G. Sandoz, in Stress Corrosion Cracking of High Strength Steels and in Aluminum and Titanium Alloys, B. F. Brown, ed., p. 79; Naval Research Lab., Washington, DC, 1974.
11. 1978 Annual Book of ASTM Standards, Vol. 10.
12. J. C. Newman, Jr., ASTM STP 560, p. 105, ASTM, Philadelphia, 1974.
13. A. M. Sullivan and T. W. Crooker, NRL Report No. 8004, Naval Research Laboratory, Washington, DC, August 1976.
14. A. D. Wilson, J. Eng. Mat. & Tech., 1979, Vol. 101, pp. 265-74.
15. C. R. Aita and J. Weertman, Met. Trans. A, 1979, Vol. 10A, pp. 535-44.
16. J. Masounave and J. P. Bailon, Scr. Met., 1976, Vol. 10, pp. 165-70.
17. K. Minakawa and A. J. McEvily, Proc. 5th Int. Conf. on the Strength of Metals and Alloys, P. Haasen, ed., Pergamon Press, New York, 1979.
18. R. O. Ritchie, MIT, Boston, MA, private communication, 1980.
19. R. O. Ritchie, MIT Fatigue and Plasticity Lab Report No. FPL/R/80/1032, MIT, Boston, MA, April 1980.
20. J. P. Benson, Metal Science, 1979, Vol. 11, pp. 535-39.

B.R.W. Hinton, University of Man
for tests with the normalised s
lar to transgranular cleavage w

H.F. Wachob: We observed a gra
 ΔK decreased from 24 MPa.m^{1/2}. F
sity, the failure mode was almo
face appears to be an inherentl
ation at this interface in both
the lowest energy form of crack
ular to intergranular when one

A. Atrons, Brown Boveri Researc
you in the very existence of a
crack growth measurements?

H.F. Wachob: The existence of
ant from an experimental and eng
probably a poor word choice. Th
the alternating stress intensit
Other researchers define "thresl
a given number of cycles where
served. In all cases, time or
riding factor for the determinat

J.P. Fidelle, Commissariat à l'É
find different fatigue threshol
process of microplastic damage,
simple reasoning is that althoug
olds should be the same unless
under high vacuum would be nece
H can affect threshold by a mecl

H.F. Wachob: We agree with you
unpublished work and from that
fatigue thresholds obtained in l
or helium) are the same. Thresl
ditions are raised above those
threshold under lab conditions
are present), an oxide debris fr
fective crack tip opening displ
alternating stress intensity. Th
the applied or observed ΔK thre
or helium. However, the effect
to that threshold value obtaine
which includes these variables
proposed by Ritchie (19). To yo
necessity for obtaining baselin
typically obtains the highest fa
vacuum. We feel that the compl
tip during fatigue under vacuum
terpretation. Therefore, we sug
be performed in high purity, we
ments; thereby eliminating the

FATIGUE CRACK GROWTH IN A516 711

DISCUSSION

B.R.W. Hinton, University of Manchester, UK: Why does the fracture mode, for tests with the normalised structure in hydrogen, change from intergranular to transgranular cleavage with increasing ΔK ?

H.F. Wachob: We observed a gradual increase of the IG mode of failure as ΔK decreased from 24 MPa.m^{1/2}. Finally, at the threshold fatigue stress intensity, the failure mode was almost entirely IG. The pearlite-ferrite interface appears to be an inherently weak interface, since we observed IG separation at this interface in both the normalized and bainitic specimens. Thus, the lowest energy form of crack propagation appears to change from transgranular to intergranular when one approaches the threshold.

A. Atrons, Brown Boveri Research Center, Baden, Switzerland: How certain are you in the very existence of a fatigue threshold stress intensity in fatigue crack growth measurements?

H.F. Wachob: The existence of a true threshold stress intensity is unimportant from an experimental and engineering standpoint. The word "threshold" is probably a poor word choice. Threshold, as defined in the present work, is the alternating stress intensity that exists at a da/dN of 10⁻⁹ m/cycle. Other researchers define "thresholds" at a given crack growth rate or after a given number of cycles where no perceptible crack extension has been observed. In all cases, time or an engineering design limit have been the overriding factor for the determination of the threshold.

J.P. Fidelle, Commissariat à l'Energie Atomique, Bruyères-le-Châtel: You find different fatigue thresholds for H₂ and air. Fatigue being a cumulative process of microplastic damage, as H₂ essentially decreases ductility, a simple reasoning is that although H₂ enhances crack growth rates, the thresholds should be the same unless oxygen has some positive effect. Experiments under high vacuum would be necessary to supply a baseline and show whether H₂ can affect threshold by a mechanism not envisioned above.

H.F. Wachob: We agree with your statement. There are indications from our unpublished work and from that of Ritchie and his co-workers (19), that the fatigue thresholds obtained in hydrogen and inert environments (either argon or helium) are the same. Thresholds obtained under typical laboratory conditions are raised above those obtained in hydrogen. When cycling near the threshold under lab conditions (i.e., where water, water vapor, and oxygen are present), an oxide debris forms near the crack tip which reduces the effective crack tip opening displacement, and therefore reduces the effective alternating stress intensity. Therefore, at the fatigue threshold in air, the applied or observed ΔK threshold is above that value obtained in hydrogen or helium. However, the effective ΔK at the crack tip is most probably equal to that threshold value obtained in hydrogen. A more comprehensive model which includes these variables as well as R ratio effects has recently been proposed by Ritchie (19). To your second comment, we strongly support the necessity for obtaining baseline fatigue threshold data. However, one typically obtains the highest fatigue threshold under conditions of a high vacuum. We feel that the complicated events such as rewelding of the crack tip during fatigue under vacuum conditions increases the difficulty of interpretation. Therefore, we suggest that baseline threshold fatigue tests be performed in high purity, well-characterized helium or other inert environments; thereby eliminating the possibility of crack tip rewelding.